

Atomic bonding and electrical characteristics of metallic and semi-metallic elements from the binding-energy and bond-charge model

Liangjing Ge, Maolin Bo*

Key Laboratory of Extraordinary Bond Engineering and Advanced Materials Technology (EBEAM) of Chongqing, Yangtze Normal University, Chongqing 408100, China

*Corresponding Author: E-mail: bmlwd@yznu.edu.cn (Maolin Bo)

Abstract

In this paper, we use density functional theory to calculate the electronic structure and properties of 47 metallic and semi-metallic elements. The binding-energy and bond-charge model (BBC) model is combined with the tight-binding and density-functional-tight-binding approaches to obtain quantitative information about atomic bonding at the atomic scale and to understand the contributions and effects of deformation energy density, energy shifts, and atomic bonding on the Hamiltonian.

Keywords: Density functional theory, Bonding states, BBC model

1. Introduction

The energies associated with the relaxation, polarization, and localization of electron wave functions near chemical bonding sites are important in the behavior of materials[1-3]. they influence crystal growth[4], decomposition[5], doping[6], adsorption[7], and catalytic reactivity[8]. The bond-order-length-strength (BOLS) correlation provides a good explanation of how atomic coordination contributes to the surface properties of a material[9,10]. Atomic systems located on surfaces have lower coordination numbers than those in bulk material and consequently different chemical and physical properties[11]. The atomic coordination number (CN) plays a key role in the relaxation of bond energy (E_i) and bond length (d_i), bonding-charge entrapment, and nonbonding polarization[12-14]. In density-functional theory (DFT), the density function of the electron $\rho(\vec{r})$, rather than the wave function, is the fundamental quantity for study[15-17]. Nevertheless, BOLS correlation describes the relaxation of chemical bonds through the CNs of atoms and does not establish a functional relationship between the electron density $\rho(\vec{r})$ and E_i [18]. We can get the exact $\rho(\vec{r})$ of the electrons in the system by doing the DFT calculation. Therefore, it is necessary to provide a DFT equivalent of BOLS correlation and establish a functional relationship between $\rho(\vec{r})$ and E_i .

The electronic structures and properties of 47 metallic or semi-metallic elements were obtained by DFT calculation. We combined binding-energy and bond-charge model (BBC) model with the density-functional-tight-binding (DFTB) approach[19] and Tight-binding (TB) model to establish a quantitative relationship between the density function of related electrons and atomic bonding. The deformation charge density was calculated by DFT to obtain quantitative information about the interatomic deformation charge-bond energy $\Delta V_{bc}(\vec{r}-\vec{r}')$, deformation atomic cohesive energy $\Delta E_{coh}(i)$, and deformation bond energy density $\Delta E_{den}(i)$. In the present study, we

obtain better predictions by combining the BBC model with the TB model and DFTB approaches.

2. Principles

2.1 DFT calculations

In this study, we applied a projection-based plane-wave DFT method[20], implemented through the Cambridge Sequential Total Energy Package (CASTEP) for material simulation at the atomic scale. We applied General Gradient Approximate (GGA)-based Perdew-Burke-Ernzerhof (PBE) functionals for the calculations[21]. **Table 1** lists the lattice parameters of metallic and semi-metallic elements; **Table 2** lists their cut-off energies and k -points. During the simulation, the energy converged to 10^{-6} eV, and the force applied to each atom converged to <0.01 eV/Å.

2.2 The DFTB and BBC models

The ground-state density is represented by a reference density, ρ_0 , around which the actual density fluctuates: $\rho(\vec{r}) = \rho_0(\vec{r}) + \delta\rho(\vec{r})$. The total energy $E[\rho_0 + \delta\rho]$ is then written as a Taylor series to the second order:

$$E[\rho_0 + \delta\rho] = E^0[\rho_0] + E^1[\rho_0 + \delta\rho] + E^2[\rho_0, (\delta\rho)^2], \quad (1)$$

where

$$\begin{aligned} E^0[\rho_0] &= \sum_i^N \varepsilon_i - \frac{1}{2} \iint \frac{\rho_0(\vec{r}) \rho_0(\vec{r}')}{|\vec{r} - \vec{r}'|} d\vec{r} d\vec{r}' - \int V^{xc}[\rho_0] \rho_0(\vec{r}) d\vec{r} + E^{xc}[\rho_0] \\ &= \sum_i \langle \phi_i | -\frac{1}{2} \nabla^2 + V_{eff}(\vec{r}) | \phi_i \rangle - \frac{1}{2} \iint \frac{\rho_0(\vec{r}) \rho_0(\vec{r}')}{|\vec{r} - \vec{r}'|} d\vec{r} d\vec{r}' - \int V^{xc}[\rho_0] \rho_0(\vec{r}) d\vec{r} + E^{xc}[\rho_0] \end{aligned}, \quad (2)$$

$$E^1[\rho_0 + \delta\rho] = Tr \left(\rho \hat{H}[\rho_0] \right) = \sum_i f_i \varepsilon_i, \quad (3)$$

and

$$E^2[\rho_0, (\delta\rho)^2] = \frac{1}{2} \iint \left\{ \frac{1}{|\vec{r} - \vec{r}'|} + \frac{\delta^2 E^{xc}}{\delta\rho(\vec{r})\delta\rho(\vec{r}')} \right\}_{\rho_0} \delta\rho(\vec{r}) \delta\rho(\vec{r}') d\vec{r} d\vec{r}' \approx \frac{1}{2} \iint \frac{1}{|\vec{r} - \vec{r}'|} \delta\rho(\vec{r}) \delta\rho(\vec{r}') d\vec{r} d\vec{r}' \quad (4)$$

In **Eq. 2**, the $E^0[\rho_0]$ is called the “repulsive energy;” it determines the dispersion of the energy band. V^{xc} and E^{xc} are the potential and exchange correlation energies, respectively; they are typically fitted from *ab initio* calculations. In **Eq. 3**, ε_i indicates the i th electronic level and f_i the corresponding electronic occupation number. In case of non-self-consistent charge DFTB, $T_r(\hat{\rho H}[\rho_0]) = \sum_i f_i \varepsilon_i$, which makes the approach equivalent to a transferable tight-binding approximation. In **Eq. 4**, we ignore the effect of the second-order fluctuations $\delta^2 E^{xc}$ of the exchange correlation energy. The $\rho_0(\vec{r})$ is the initial density function, and $\delta\rho(\vec{r})$ is the deformation density function.

If we consider the effect of charge transfer on binding energy shifts, combining the BBC model with the DFTB model, we obtain:

$$\begin{aligned} E[\rho_0 + \delta\rho] &= E^0[\rho_0] + E^1[\rho_0 + \delta\rho] + E^2[\rho_0, (\delta\rho)^2] \\ &\approx \left(\sum_i^N \varepsilon_i - \frac{1}{2} \iint \frac{\rho_0(\vec{r}) \rho_0(\vec{r}')}{|\vec{r} - \vec{r}'|} d\vec{r} d\vec{r}' - \int V^{xc}[\rho_0] \rho_0(\vec{r}) d\vec{r} + E^{xc}[\rho_0] \right) + \sum_i f_i \varepsilon_i + \frac{1}{2} \iint \frac{1}{|\vec{r} - \vec{r}'|} \delta\rho(\vec{r}) \delta\rho(\vec{r}') d\vec{r} d\vec{r}' \end{aligned} \quad (5)$$

The second term $E^1[\rho_0 + \delta\rho]$, which represents the contribution of the external field to the Hamiltonian, determines the relative energy-level shift $\Delta E'_v(x)$. Without the effect of the external field, the second term does not contribute to the Hamiltonian.

From the Eq.3, the combined DFTB [22,23], we have:

$$\Delta V_{bc}(\vec{r} - \vec{r}') = \frac{1}{8\pi\epsilon_0} \int d^3r \int d^3r' \frac{\delta\rho(\vec{r})\delta\rho(\vec{r}')}{|\vec{r} - \vec{r}'|},$$

(6)

where ϵ_0 is the dielectric constant of vacuum. Also, $\delta\rho$ satisfies the following relationship

$$(\delta\rho_{Hole-electron} < \delta\rho_{Antibonding-electron} < \delta\rho_{No charge transfer} = 0 < \delta\rho_{Nonbonding-electron} < \delta\rho_{Bonding-electron})$$

(7)

For atomic (strong) bonding states:

$$\delta\rho_{Hole-electron}(\vec{r})\delta\rho_{Bonding-electron}(\vec{r}') < 0 (Strong Bonding).$$

(8)

For atomic nonbonding or weak-bonding states:

$$\begin{aligned} \delta\rho_{Hole-electron}(\vec{r})\delta\rho_{Nonbonding-electron}(\vec{r}') &< 0 (Nonbonding or Weak Bonding) \\ \delta\rho_{Antibonding-electron}(\vec{r})\delta\rho_{Bonding-electron}(\vec{r}') &< 0 (Nonbonding or Weak Bonding) \\ \delta\rho_{Antibonding-electron}(\vec{r})\delta\rho_{Nonbonding-electron}(\vec{r}') &< 0 (Nonbonding) \end{aligned}$$

(9)

For atomic antibonding states:

$$\begin{aligned} \delta\rho_{Nonbonding-electron}(\vec{r})\delta\rho_{Bonding-electron}(\vec{r}') &> 0 (Antibonding) \\ \delta\rho_{Hole-electron}(\vec{r})\delta\rho_{Antibonding-electron}(\vec{r}') &> 0 (Antibonding) \\ \delta\rho_{Hole-electron}(\vec{r})\delta\rho_{Hole-electron}(\vec{r}') &> 0 (Antibonding) \\ \delta\rho_{Antibonding-electron}(\vec{r})\delta\rho_{Antibonding-electron}(\vec{r}') &> 0 (Antibonding) \\ \delta\rho_{Nonbonding-electron}(\vec{r})\delta\rho_{Nonbonding-electron}(\vec{r}') &> 0 (Antibonding) \\ \delta\rho_{Bonding-electron}(\vec{r})\delta\rho_{Bonding-electron}(\vec{r}') &> 0 (Antibonding) \end{aligned}$$

(10)

From the Hubbard model[24], we get

$$\begin{aligned}\hat{V}_{bc} &= \frac{1}{2} \int d^3r \int d^3r' \alpha_\sigma^+(\vec{r}) \alpha_\sigma(\vec{r}) V_{ee}(\vec{r} - \vec{r}') \alpha_{\sigma'}^+(\vec{r}') \alpha_{\sigma'}(\vec{r}') \\ &= \frac{1}{4\pi\epsilon_0} \frac{1}{2|\vec{r} - \vec{r}'|} \int d^3r \int d^3r' \rho(\vec{r}) \rho(\vec{r}')\end{aligned}\quad (11)$$

where $\alpha_\sigma(\vec{r})$ and $\alpha_\sigma^+(\vec{r})$ are annihilation and creation operators, respectively. For the sake of completeness, we have endowed the electrons with a spin index, $\sigma = \uparrow/\downarrow$. The charge density is $\rho(\vec{r}) = \sum_i e_i \alpha_\sigma^+(\vec{r}) \alpha_\sigma^-(\vec{r})$. The quantity $V_{ee}(\vec{r} - \vec{r}') = \frac{1}{4\pi\epsilon_0} \frac{\sum_i e_i \sum_j e_j}{2|\vec{r}_i - \vec{r}'_j|}$ is the potential of the electron, which induces a transformation

$$\alpha_\sigma^+(\vec{r}) = \sum_{\vec{R}} \psi_{\vec{R}}^*(\vec{r}) a_{\vec{R}\sigma}^+ \equiv \sum_i \psi_{\vec{R}i}^*(\vec{r}) a_{i\sigma}^+ . \quad (12)$$

Inserting (11) into (10) leads to the expansion $\hat{V}_{bc} = \sum_{ii'jj'} U_{ii'jj'} a_{i\sigma}^+ a_{i'\sigma}^+ a_{j\sigma}^- a_{j'\sigma}^-$, where $U_{ii'jj'} = \frac{1}{2} \int d^3r \int d^3r' \psi_{\vec{R}i}^*(\vec{r}) \psi_{\vec{R}j}(\vec{r}) V_{ee}(\vec{r} - \vec{r}') \psi_{\vec{R}i'}^*(\vec{r}') \psi_{\vec{R}j'}(\vec{r}')$

is the Coulomb interaction.

2.3 TB model, BOLS correlation, and BBC model

The TB model leads to the formulas

$$H = -\frac{\hbar^2 \nabla^2}{2m} + V_a(\vec{r}) + V_c(\vec{r})(1 + \Delta_H), \quad (14)$$

$$\left\{ \begin{array}{l} E_v(0) = -\langle \phi_v(\vec{r}) | -\frac{\hbar^2 \nabla^2}{2m} + V_a(\vec{r}) | \phi_v(\vec{r}) \rangle \\ E_v(x) - E_v(0) = -\langle \phi_v(\vec{r}) | V_c(\vec{r}) | \phi_v(\vec{r}) \rangle \left[1 + \frac{\sum_j f(k) \langle \phi_v(\vec{r}) | V_c(\vec{r} - \vec{R}) | \phi_v(\vec{r} - \vec{R}) \rangle}{\langle \phi_v(\vec{r}) | V_c(\vec{r}) | \phi_v(\vec{r}) \rangle} \right], \\ = \alpha_v (1 + \sum_j \frac{e^{ik(\vec{r}-\vec{R})} \cdot \beta_v}{\alpha_v}) \cong \alpha_v (1 + \Delta_H) \propto \langle E_x \rangle \end{array} \right. \quad (15)$$

$$\alpha_v = -\langle \phi_v(\vec{r}) | V_c(\vec{r}) | \phi_v(\vec{r}) \rangle \propto \langle E_b \rangle; \quad \beta_v = -\langle \phi_v(\vec{r}) | V_c(\vec{r} - \vec{R}) | \phi_v(\vec{r} - \vec{R}) \rangle; \quad \Delta_H = \sum_j \frac{f(k) \cdot \beta_v}{\alpha_v} \cong \delta\gamma \quad (16)$$

Here, $E_v(x)$ is the v -th energy level of a crystal atom, and $E_v(0)$ is the v -th energy level of an isolated atom; $V_a(\vec{r})$ and $V_c(\vec{r})$ are the potential energies of the atom and crystal, respectively. Both α_v and β_v in **Eq. 15** contribute to the energy band width. However, the energy band of the core energy level is determined by α_v , because β_v is very small in the local energy band of the core energy level. The wave function is

$$\psi_v(\vec{r}) = \frac{1}{\sqrt{N}} \sum_l e^{ik\vec{R}} \phi(\vec{r} - \vec{R}); \text{ the form of the periodic factor } f(k) \text{ is } e^{ik(\vec{r}-\vec{R})}, \text{ where } k$$

represents the wave vector. The quantity β depends on the overlap between orbitals centered at two neighboring atoms; \vec{r} is the radius of the electron.

The inner electrons are affected by the potential energy of the crystal, which causes shifts in the core energy levels. Combining initial- and final-state effects with the Tight-binding model, we obtain[25]:

$$\left\{ \begin{array}{l} V_c(\vec{r})(1 + \Delta_H) = \gamma V_c(\vec{r}) = (1 + Z)V_c(\vec{r}) \\ V_a(r) = -\frac{1}{4\pi\epsilon_0} \frac{ze^2}{r}, \quad V_c(\vec{r}) = -\sum_{l, \vec{R}_l \neq 0} \frac{1}{4\pi\epsilon_0} \frac{ze^2}{|\vec{r} - \vec{R}_l|} \end{array} \right. \quad (17)$$

$$E_v(x) - E_v(0) \cong -\langle \phi_v(r) | V_c(\vec{r})(1 + \Delta_H) | \phi_v(r) \rangle = -(1 + Z) \langle \phi_v(r) | V_c(\vec{r}) | \phi_v(r) \rangle \propto \langle E_x \rangle, \quad (18)$$

$$E_v(x) - E_v(B) \cong -\delta\gamma \langle \phi_v(r) | V_c(\vec{r}) | \phi_v(r) \rangle \cong -\sum_j f(k) \langle \phi_v(\vec{r}) | V_c(\vec{r} - \vec{R}) | \phi_v(\vec{r} - \vec{R}) \rangle,$$

(19)

where Z represents the atomic charge parameter; $\gamma = Z + 1$ and $\delta\gamma = \gamma - 1$ are the binding-energy ratio and relative binding-energy ratio, respectively, and B indicates bulk atoms.

For convenience of calculation, the atomic ion is taken to have $Z = 1$. The energy-level shifts in an external field obtained from Eqs. 16, 17 and 18 are:

$$Z = -1 (\delta\gamma = -1, \gamma = 0, \text{Nonbonding}), \Delta E_v(x) = \Delta E_v(0) = 0 \quad (\text{isolated atom, neutral atom}) \quad (20)$$

$$Z = 0 (\delta\gamma = 0, \gamma = 1, \text{Bonding}), \Delta E_v(x) = \Delta E_v(B) = -\left(-\sum_{l, R_l \neq 0} \langle v, i | \frac{1}{4\pi\varepsilon_0} \frac{e^2}{|\vec{r} - \vec{R}_l|} |v, i\rangle\right) > 0 \quad (\text{bulk atoms, charged positive atoms}) \quad (21)$$

$$Z = |\delta\gamma| (\delta\gamma > 0, \text{Bonding}), \Delta E_v(x) = -\left(-\langle v, i | \sum_{l, R_l \neq 0} \frac{(1+|\delta\gamma|)}{4\pi\varepsilon_0} \frac{e^2}{|\vec{r} - \vec{R}_l|} |v, i\rangle\right) > 0 \quad (\text{charged positive atoms}) \quad (22)$$

$$Z = -|\delta\gamma| (\delta\gamma < 0) \begin{cases} -1 < \delta\gamma < 0, \text{Nonbonding}, \Delta E_v(x) = -\left(-\sum_{l, R_l \neq 0} \langle v, i | \frac{(1-|\delta\gamma|)}{4\pi\varepsilon_0} \frac{e^2}{|\vec{r} - \vec{R}_l|} |v, i\rangle\right) > 0 \\ \delta\gamma < -1, \text{Antibonding}, \Delta E_v(x) = -\left(-\sum_{l, R_l \neq 0} \langle v, i | \frac{(1-|\delta\gamma|)}{4\pi\varepsilon_0} \frac{e^2}{|\vec{r} - \vec{R}_l|} |v, i\rangle\right) < 0 \end{cases} \quad (\text{charged negative atoms}) \quad (23)$$

Energy-level shifts reflect bond changes and electron transfers. Through DFT calculations and X-ray photoelectron spectroscopy (XPS) analysis, we can pass the known reference values $\Delta E'_v(x) = E_v(x) - E_v(B)$, $\Delta E_v(B) = E_v(B) - E_v(0)$, and $\Delta E_v(x) = E_v(x) - E_v(0)$ to calculate the relative binding-energy ratio $\delta\gamma$ induced by the external field:

$$\delta\gamma = \frac{\Delta E'_v(x)}{\Delta E_v(B)} \approx \frac{\Delta E'_v(x)}{2\Delta E_v(\text{FWHM})}, \quad (24)$$

where FWHM indicates the full widths at half maximum of the measured spectral

peaks. If $\delta\gamma < 0$, the atom gains electrons and the binding energy is reduced: the potential energies of crystals and chemical bonds are weakened. Conversely, if $\delta\gamma > 0$, the atom loses electrons and the binding energy increases: the bond and the potential of the crystal become stronger.

The properties of chemical bonds can be obtained in terms of the binding-energy ratio γ . Combining the BOLS correlation, we obtain:

$$C_i(z_i) = d_i / d_b = 2 \left\{ 1 + \exp \left[(12 - z_i) / (8z_i) \right] \right\}^{-1} \quad (\text{bond contraction coefficient}) \quad (25)$$

$$z_i = \frac{12}{8 \ln \left(\frac{2\Delta E'_v(x) - \Delta E_v(B)}{\Delta E_v(B)} \right) + 1} \quad (\Delta E_v(x) \geq 0) \quad (\text{coordination number}) \quad (26)$$

$$\gamma = \frac{\Delta E'_v(x)}{\Delta E_v(w_B)} = \frac{\Delta E'_v(x) + \Delta E_v(B)}{\Delta E_v(B)} \quad (\text{binding energy ratio}) \quad (27)$$

$$\begin{cases} E_i = C_i^{-m} E_b & (\text{bond strengthening}) \\ \varepsilon_i = d_i / d_b - 1 = \gamma^{-1} - 1 & (\text{local bond strain}) \\ \delta E_{den}(i) = (E_i / d_i^3) / (E_b / d_b^3) - 1 = \gamma^{3+m} - 1 & (\text{relative bond energy density}) \\ \delta E_{coh}(i) = z_i E_i / z_b E_b - 1 = z_{ib} \gamma^m - 1 & (\text{relative atomic cohesive energy}) \\ E_{surf}(i) = N_i E_{coh}(i) = N \chi_i z_i E_i & (\text{surface cohesive energy}) \end{cases} \quad (28)$$

$$\begin{cases} E_v(i) = E_v(0) + \Delta E_v(B) C_i^{-m} & (\text{surface effect}) \\ \Delta E_i = \int d^3 r \int d^3 r' \frac{\delta \rho(\vec{r}) \delta \rho(\vec{r}')}{4\pi \epsilon_0 d_i} & (\text{relative bond energy}) \\ E_v(K) = E_v(B) + \Delta E_v(B) \left[\tau K^{-1} \sum_{i \leq 3} C_i (C_i^{-m} - 1) \right] = E_v(B) + \Delta E_v(B) \left[1.69 N^{-1/3} \tau \sum_{i \leq 3} C_i (C_i^{-m} - 1) \right] & (\text{size effect}) \\ E_v(T) = E_v(B) + \Delta E_v(B) \frac{9R}{E_{coh}} \left(\frac{T}{\theta_D} \right)^4 \int_0^T \int_0^{\theta_D/T} \frac{x^4 e^x}{(e^x - 1)^2} dx dt & (\text{thermal effect}) \end{cases} \quad (29)$$

where $C_i(z_i)$ represents the coefficient of bond contraction, with z_i being the effective coordination of an atom in the i th atomic layer; N is the number of atoms; and

K is the nanoparticle radius. $E_{\text{coh}}(i)$ is the cohesive energy of the atoms; $E_{\text{den}}(i)$ is the bond energy density; $\chi = N_i / N$ is the specific surface area; τ is the shape factor of the nanoparticles; θ_D represents the Debye temperature; and m is the bond performance parameter ($m = 1$ for metal).

3. Results and discussion

3.1. Structural characteristics and electronic properties of metallic and semi-metallic elements

We used DFT to calculate the properties of 47 metallic and semi-metallic elements. The geometric initial structures of the 47 elements are shown in **Fig. 1**, and their lattice constants in **Table 1**. It can be seen from **Fig. 1** that C, Si, Ge, and Sn have diamond structures; Li, Na, K, V, Cr, Fe, Rb, Nb, Mo, In, Cs, Ba, Ta, and W have body-centered cubic (bcc) structures; Be, Mg, Sc, Ti, Zn, Y, Zr, Tc, Ru, Cd, Lu, Hf, Re, Os, and Tl have hexagonal close-packed (hcp) structures; and Al, Ca, Co, Ni, Cu, Sr, Rh, Pd, Ag, Ir, Pt, Au, and Pb have faced-centered cubic (fcc) structures. The bonds formed by these elements are metallic. The diamond-structure elements form covalent bonds through the valence electrons of surrounding atoms. Note that As has a rhomb structure. Each layer is held together internally by strong covalent (σ) bond; these layers are then linked by weak van der Waals forces (π bonds).

The energy-orbital distribution is very important for metallic and semi-metallic physical systems and directly determines their electronic properties. We calculated the partial density of states (PDOS) of the 47 elements (**Fig. 2**); their cut-off energies are given in **Table 2**. For metals, electrons do not have zero energy at the Fermi surface ($E_F \neq 0$). From **Fig. 2**, we can see that the d -orbital PDOSs of Ca, Sc, Ti, V, Cr, Fe, Co, Ni, Sr, Y, Zr, Nb, Mo, Tc, Ru, Rh, Pd, Ba, Hf, Ta, W, Re, Os, Ir, and Pt had obvious fluctuations and spikes near the Fermi surface. This shows that the d electrons were relatively localized, and the main contribution to the structural energy was from the d orbital. The IA and IIA elements Cu, Zn, Ag, Cd, and Au had small fluctuations near the Fermi surface and large ones on its left side; they were relatively smooth near the Fermi level, with comparatively strong non-local properties. The d orbitals of Li, Be,

C, Na, Mg, Al, Si, K, Ge, As, Rb, In, Sn, Cs, Lu, Tl, and Pb contributed very little. In addition, the elements with diamond structure had semiconductor properties; in them, there was no electron distribution near the Fermi level, and there were obvious band gaps. From **Fig. 3**, the band gaps of C, Si, and Ge were 4.396 eV, 0.710 eV, and 0.181 eV, respectively.

3.2 Atomic bonding-electron states and deformation charge density

DFT was used to calculate $\Delta\rho(r)$ for 47 metallic and semi-metallic elements (**Fig. 4**). Charge density concentrated around an atom may represent the formation of ionic bonds; atoms rely on free electrons to produce strong interactions for metallic or covalent bonds. Elements with the same lattice structure tend to have similar electronic bonding states. Here, we analyze the electron bonding states using the BBC model. From the charge transfer process of the deformation charge-density diagram, we obtain the electronic states of chemical bonds of various elements.

Given $\Delta\rho(r)$, we use the BBC model to obtain the relevant bonding value. **Table 3** lists the bonding-state deformation charge densities $\delta\rho^{Bonding-electron}(\vec{r}')$ $\left(e/\text{\AA}^3\right)$ of each element determined by DFT calculation, the atomic bond length d , and $\Delta V_{bc}(\vec{r}-\vec{r}')$, where $V_{bc}(\vec{r}-\vec{r}')$ is the potential energy of electron exchange. **Eq. 6** describes the relationship between $\Delta\rho(r)$ and $\Delta V_{bc}(\vec{r}-\vec{r}')$; for crystal structures, the latter depends on the electron densities of the different bonding electronic states. In **Fig. 5**, we show how $\Delta V_{bc}(\vec{r}-\vec{r}')$ changed for the 47 metals and semi-metals across the periodic table. The deformation charge-bond energies of metallic and semi-metallic elements in the same group decreased gradually from top to bottom of a column (except in the case of carbon, a chemically active element).

From **Eq. 6**, **Eq. 28**, and **Eq. 29**, using to the $\Delta\rho(r)$ obtained from the DFT calculation, we can calculate:

$$\begin{cases} \Delta E_{coh}(i) = z_i \int d^3r \int d^3r' \frac{\delta\rho(\vec{r})\delta\rho(\vec{r}')}{4\pi\varepsilon_0 d_i} = \frac{z_i}{4\pi\varepsilon_0 d_i} \int d^3r \int d^3r' \delta\rho(\vec{r})\delta\rho(\vec{r}') \\ \Delta E_{den}(i) = \frac{1}{d_i^3} \int d^3r \int d^3r' \frac{\delta\rho(\vec{r})\delta\rho(\vec{r}')}{4\pi\varepsilon_0 d_i} = \frac{1}{4\pi\varepsilon_0 d_i^4} \int d^3r \int d^3r' \delta\rho(\vec{r})\delta\rho(\vec{r}') \end{cases} \quad (30)$$

From **Eq. 30**, we obtained the results shown in **Table 4**. **Fig. 6** shows $\Delta E_{coh}(i)$ and $\Delta E_{den}(i)$ for the 47 elements arranged by atomic number. The sign of $\Delta E_{coh}(i)$ for the atoms determines the thermal stability[26]. In addition, we compared the $\Delta E_{coh}(i)$ and cohesive energies of metals and semi-metals as is show in **Fig. 6a**. The value of $\Delta E_{den}(i)$ indicates that the mechanical properties of the material[27]. We compared the $\Delta E_{den}(i)$ and atomic concentration of metals and semi-metals, as is show in **Fig. 6b**. We find that the calculated deformation atomic cohesive energy $\Delta E_{coh}(i)$ and deformation bond energy density $\Delta E_{den}(i)$ are consistent with the trend of cohesive energies and atomic concentration. Atomic concentration and cohesive energies value are from the ref[28]. Considering the complex electronic structure system of heavy elements, we did not calculate the $\Delta E_{den}(i)$ and $\Delta E_{coh}(i)$ of the heavy element system.

4. Conclusions

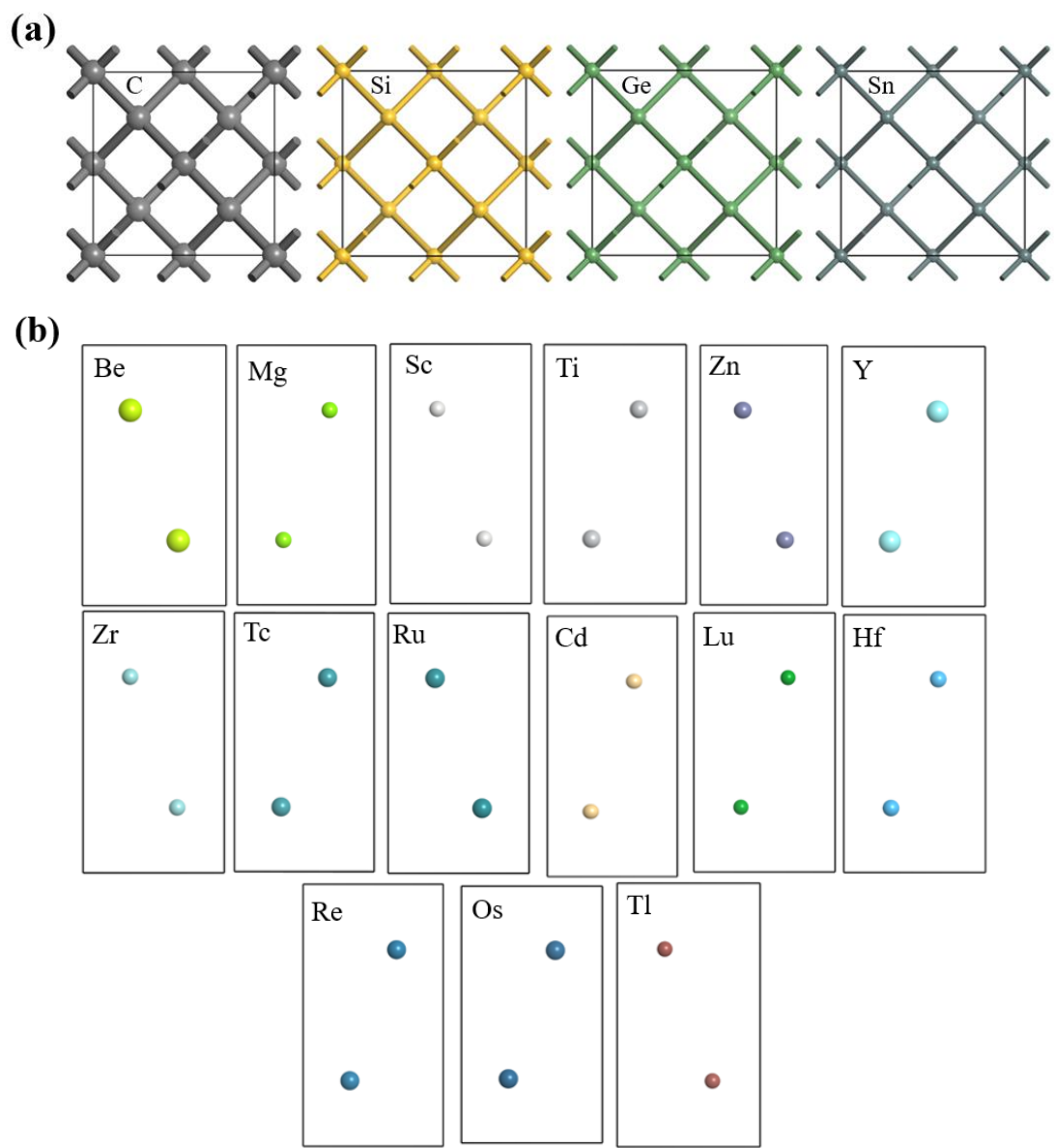
We used DFT to calculate the electronic properties and bonding states of 47 metallic and semi-metallic elements. The BBC model provided a quantitative relationship between the density function of relevant electrons and of chemical bonds. Through DFT calculation, we obtained quantitative information about $\Delta V_{bc}(\vec{r} - \vec{r}')$, which determines the electronic bonding state; $E_{coh}(i)$, which determines the thermal stability of the material; and $E_{den}(i)$, which determines the mechanical properties. This can provide better theoretical understanding of atomic bonding states and charge

transfer in metallic and semi-metallic elements.

References

- [1] Putz, V. Mihai, Int. J. Mol. Sci. **2008**, 9, 1050.
- [2] M. Magnuson, M. Mattesini, Thin Solid Films **2017**, 621, 108.
- [3] Ruedenberg, Klaus, Schmidt, W. Michael, J. Phys. Chem. A **2009**, 113, 1954.
- [4] H. Tominaga, M. Sakai, T. Fukuda, T. Namikata, J. Cryst. Growth **1974**, 272, 24.
- [5] M. Raupach, R. Tonner, J. Chem. Phys. **2015**, 142, 194105.
- [6] P.E. Lippens, A.V. Chadwick, A. Weibel, R. Bouchet, P. Knauth, J. Phys. Chem. C **2008**, 112, 43.
- [7] C. Hogan, D. Paget, Y. Garreau, M. Sauvage, G. Onida, L. Reining, P. Chiaradia, V. Corradini, Phys. Rev. B **2003**, 68, 205313.
- [8] F. Cuminet, S. Caillol, É. Dantras, É. Leclerc, V. Ladmiral, Macromol. **2021**, 54, 3927.
- [9] J. Zhou, M. Bo, L. Li, Z. Huang, M. Tian, C. Yao, C. Peng, Adv. Theory Simul. **2018**, 8, 1800035.
- [10] M. Bo, L. Li, Y. Guo, C. Yao, C.Q. Sun, Appl. Surf. Sci. **2018**, 427, 1182.
- [11] Weidenbruch, Manfred, J. Organomet. Chem. **2002**, 646, 39.
- [12] D. Prof., R. Hoppe, Angew. Chem. **1970**, 9, 25.
- [13] A. Ferté, F. Penent, J. Palaudoux, H. Iwayama, E. Shigemasa, Y. Hikosaka, K. Soejima, P. Lablanquie, R. Taïeba, S. Carniato, Phys. Chem. Chem. Phys. **2022**, 2, 597.
- [14] D. Wu, C. Xi, C. Dong, H. Liu, X.-W. Du, J. Phys. Chem. C **2019**, 123, 28248.
- [15] R.G. Parr, Ann. rev. phys. chem. **1983**, 34, 631.
- [16] Vener, M.V. Egorova, A.N. Churakov, A.V. Tsirelson, V. G., Comput.Chem. **2012**, 33, 2303.
- [17] K.Nakada, A.Ishii, Solid State Commun. **2011**, 151, 13.
- [18] X. Zhang, T. Yan, Y. Huang, Z. Ma, X. Liu, B. Zou, C.Q. Sun, Phys. Chem. Chem. Phys. **2014**, 16, 24666.
- [19] B. Hourahine, B. Aradi, V. Blum, F. Bonafé, A. Buccheri, C. Camacho, C. Cevallos, M.Y. Deshaye, T. Dumitrică, A. Dominguez, S. Ehlert, M. Elstner, T.v.d. Heide, J. Hermann, S. Irle, J.J. Kranz, C. Köhler, T. Kowalczyk, T. Kubář, I.S. Lee, V. Lutsker, R.J. Maurer, S.K. Min, I. Mitchell, C. Negre, T.A. Niehaus, A.M.N. Niklasson, A.J. Page, A. Pecchia, G. Penazzi, M.P. Persson, J. Řezáč, C.G. Sánchez, M. Sternberg, M. Stöhr, F. Stuckenber, A. Tkatchenko, V.W.z. Yu, T. Frauenheim, J. Chem. Phys. **2020**, 152, 124101.
- [20] D. Benjamin, Dunnington, J.R.Schmidt, J. Chem. Phys. **2015**, 143, 104109.
- [21] B. Hammer, L.B. Hansen, J.K. Nørskov, Phys. Rev. B **1999**, 59, 7413.
- [22] M. Bo, H. Li, A. Deng, L. Li, C. Peng, Mater. Adv. **2020**, 1, 1186.
- [23] M. Bo, H. Li, Z. Huang, L. Li, C. Yao, AIP Adv. **2020**, 10, 015321.
- [24] V. Bach, E.H. Lieb, J.P. Solovej, J. Stat. Phys. **1994**, 76, 3.
- [25] H. Qiu, H. Li, J. Wang, Y. Zhu, M. Bo, Phys. Status Solidi L **2022**, 16, 2100444.
- [26] C.Q. Sun, Prog. Mater. Sci. **2009**, 54, 179.
- [27] C.Q. Sun, Prog. Solid State Chem. **2007**, 35, 1.
- [28] C. Kittel, P. McEuen, Introduction to Solid State Physics[M], John Wiley & Sons, **2018**.

Figure and Table Captions



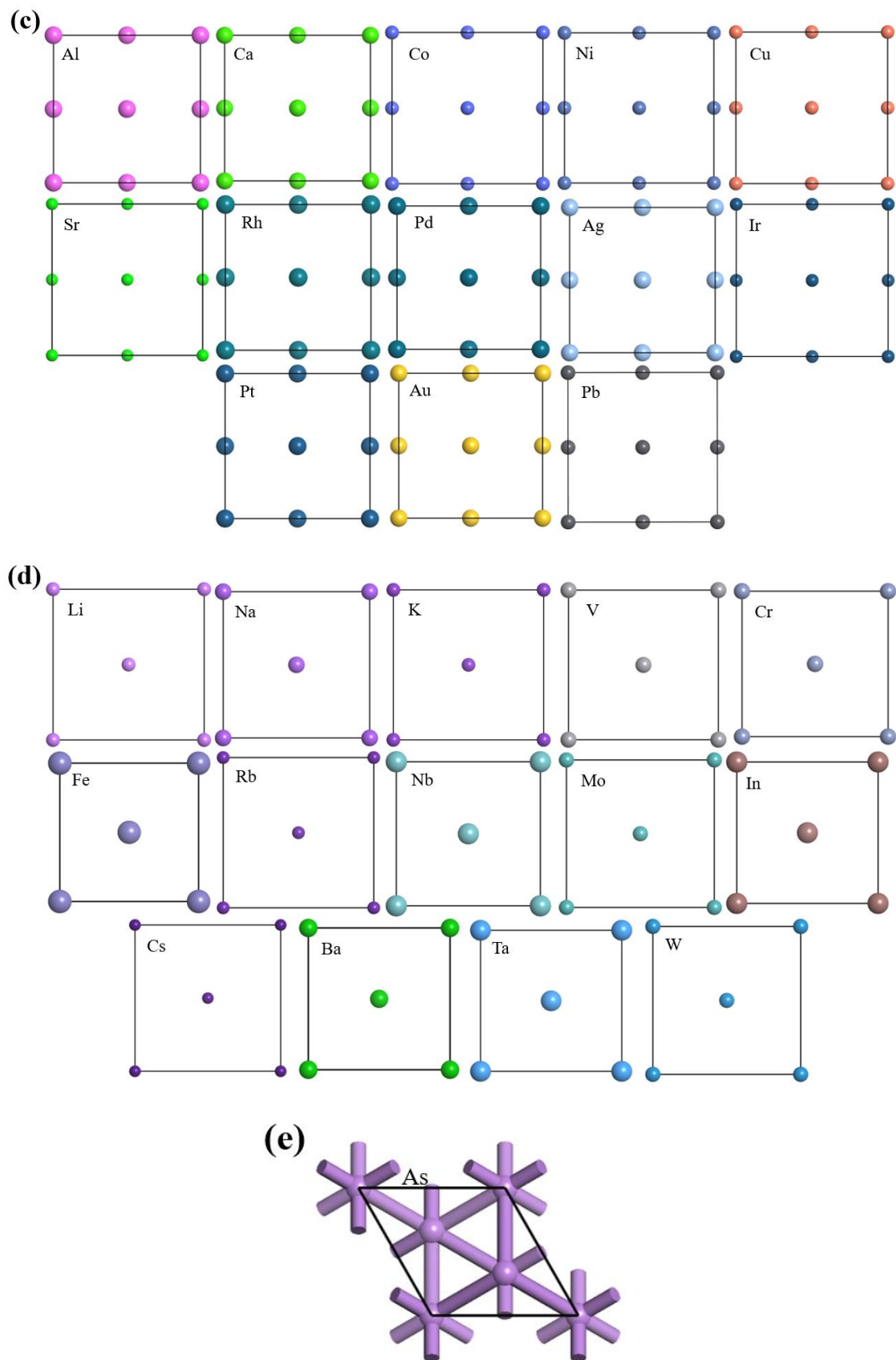
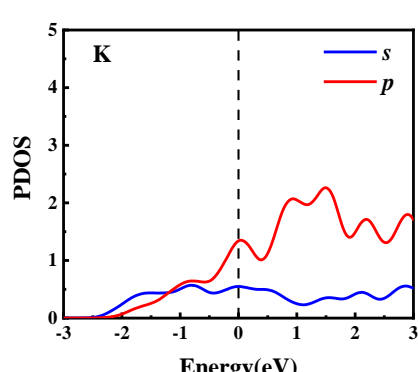
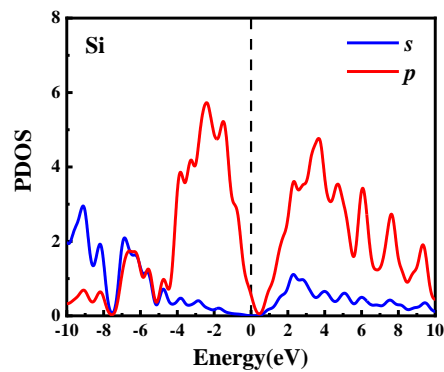
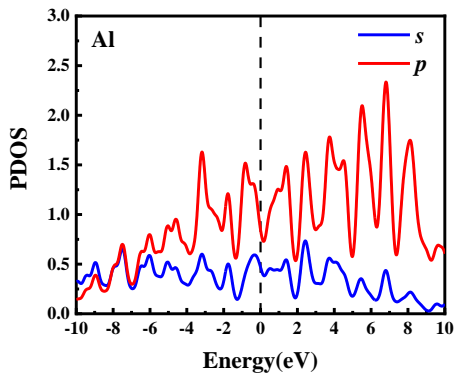
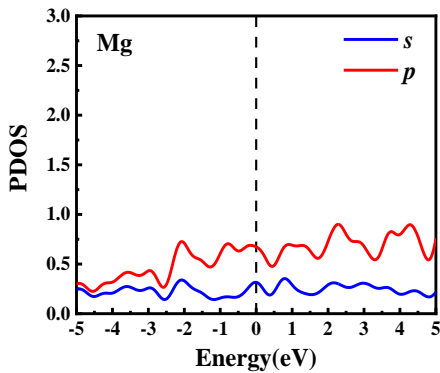
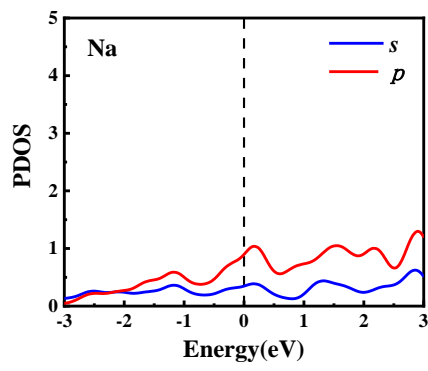
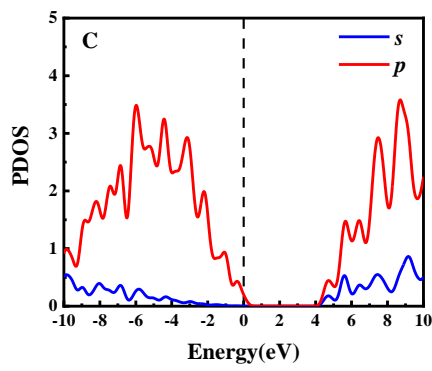
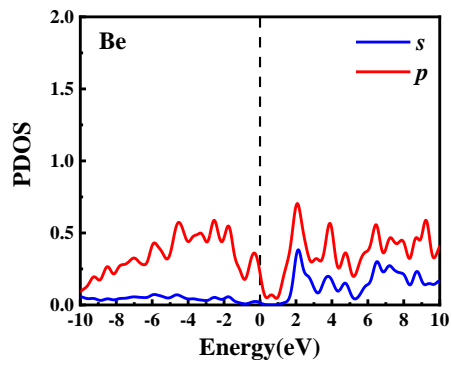
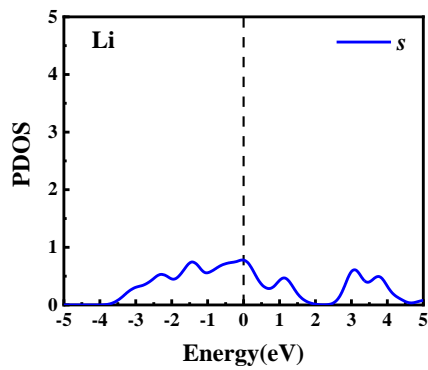
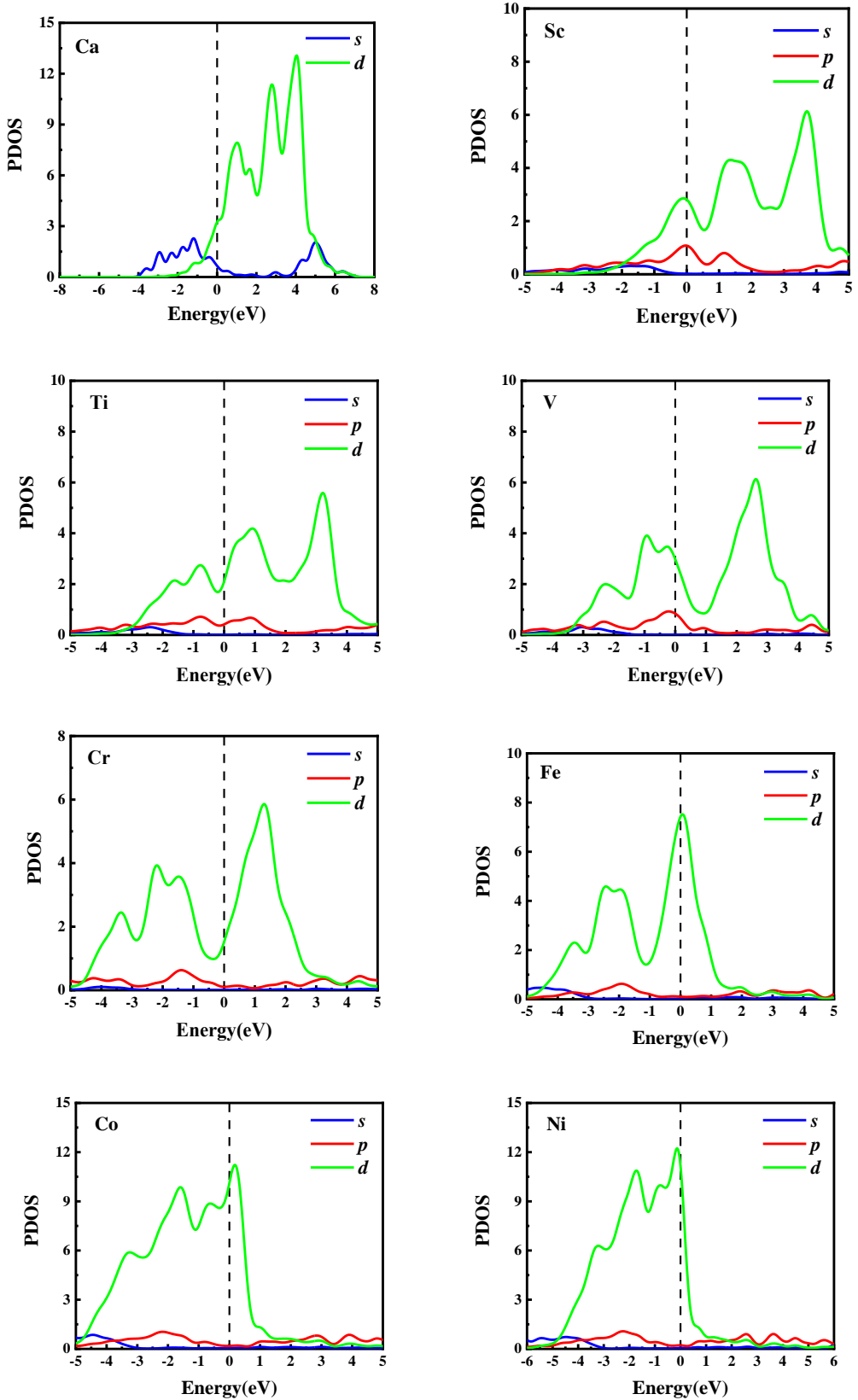
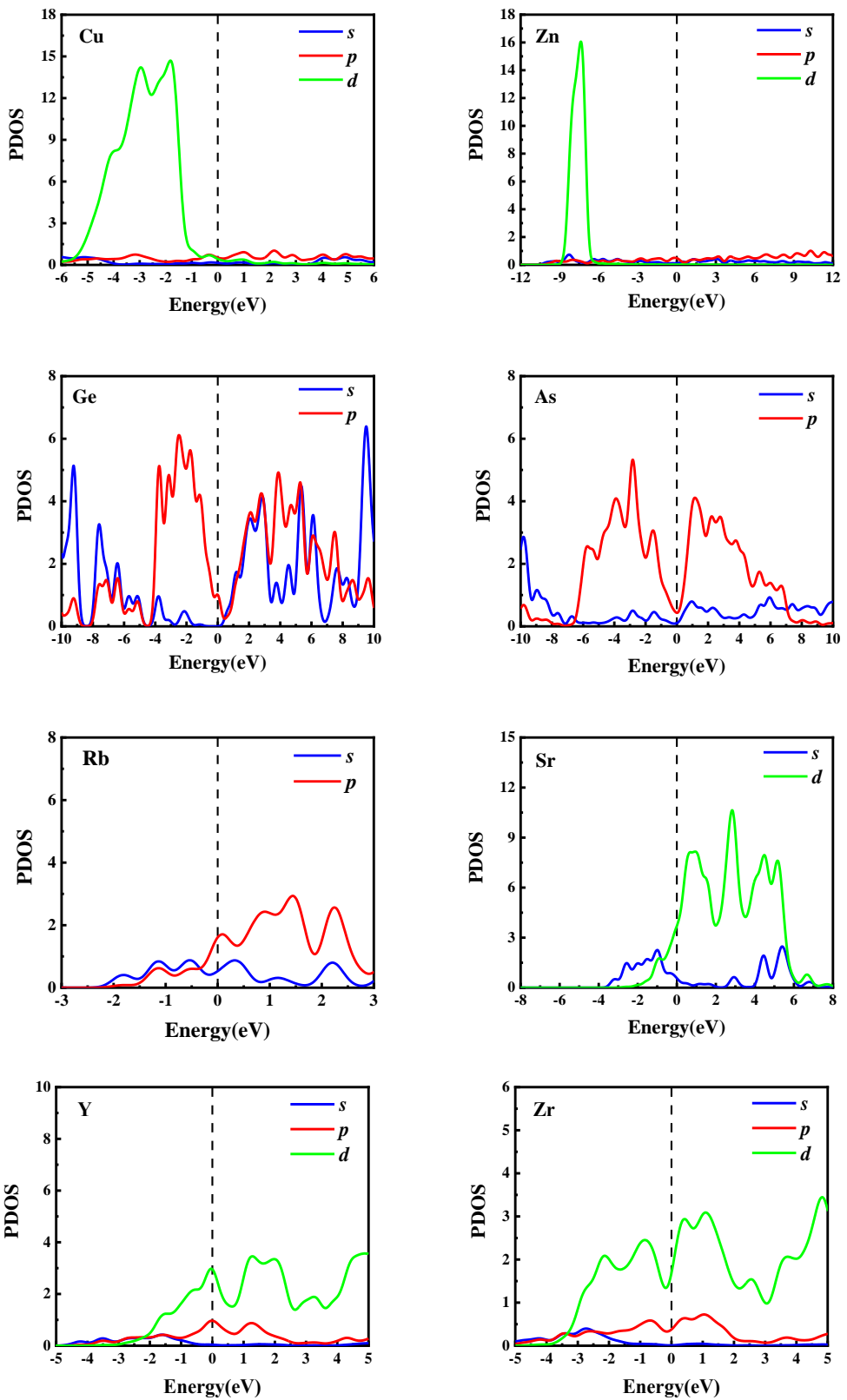
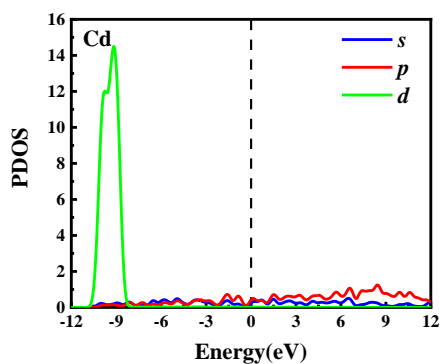
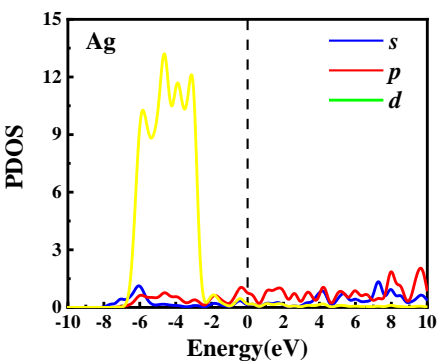
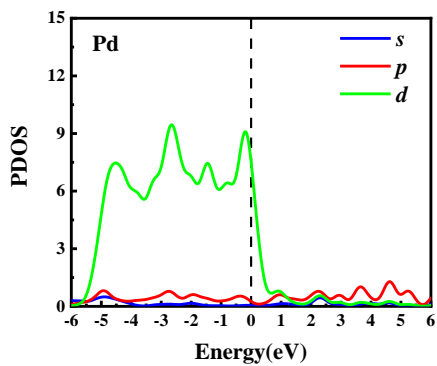
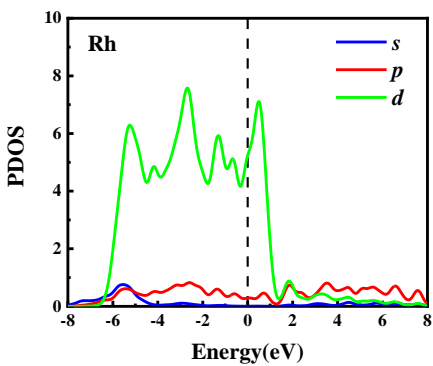
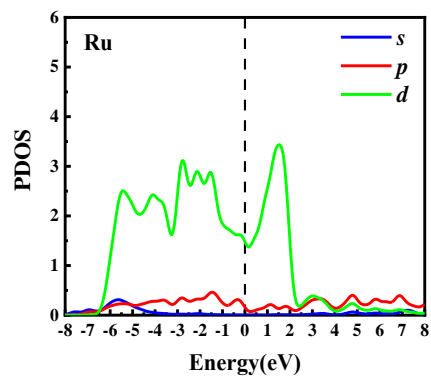
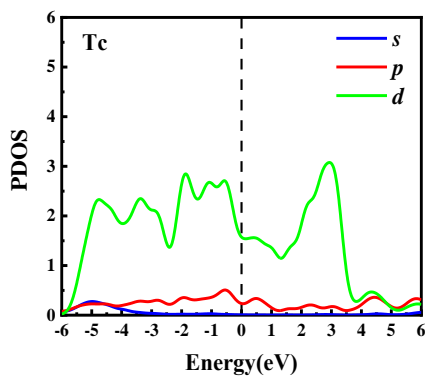
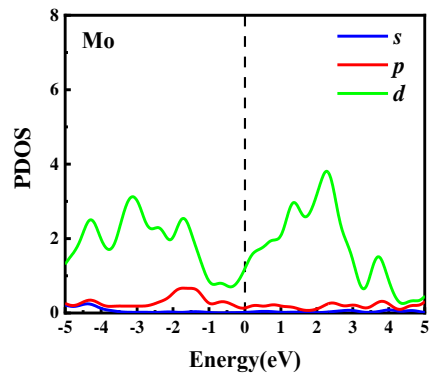
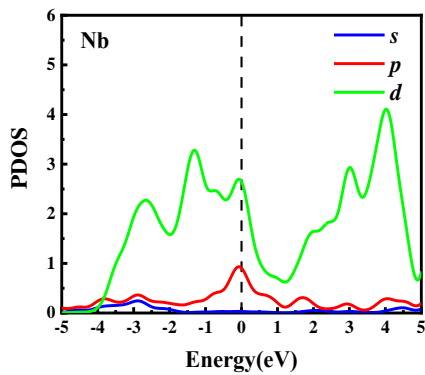


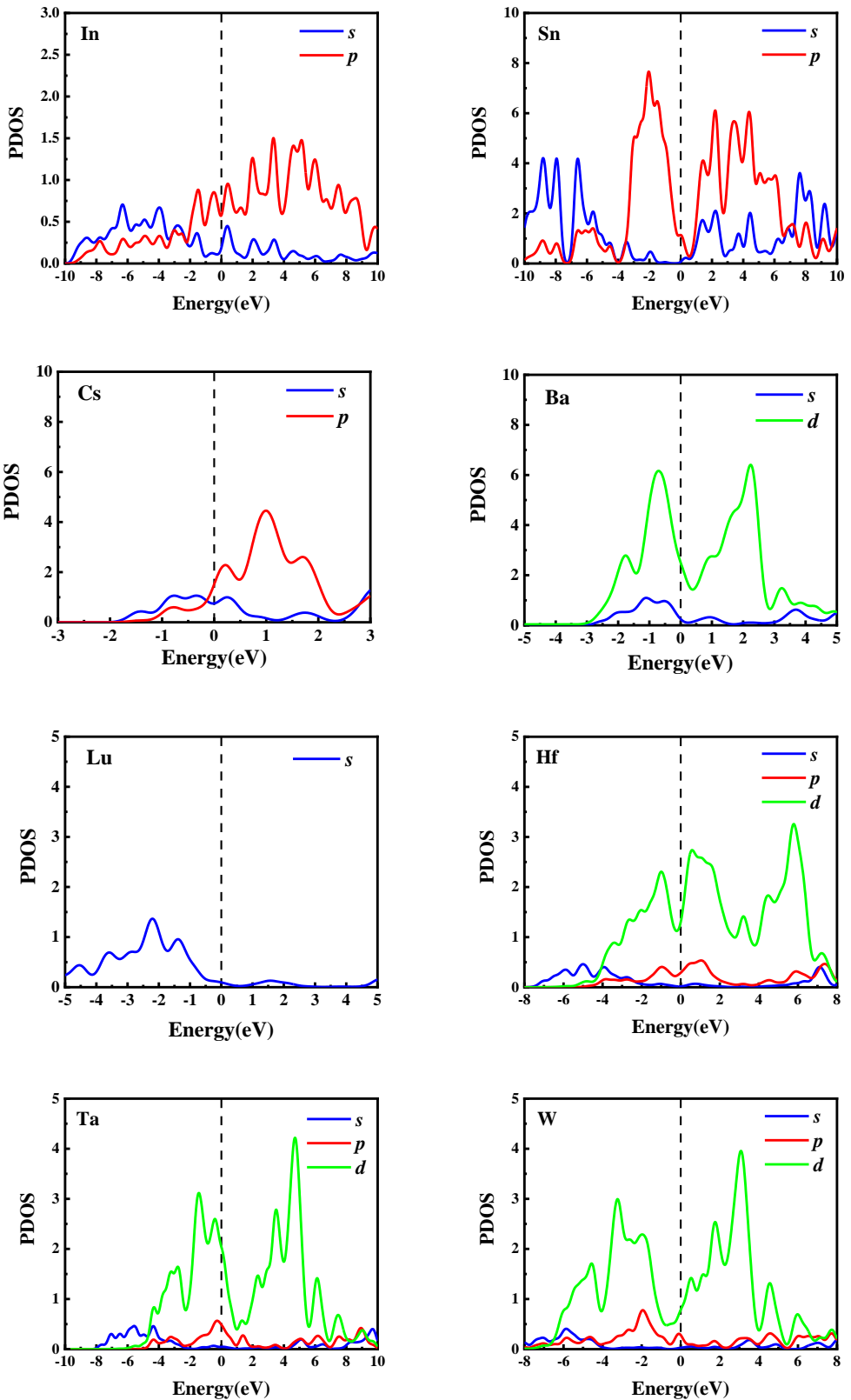
Fig. 1 Initial geometric structures of 47 metallic and semi-metallic elements: (a) diamond structure; (b) hcp structure; (c) fcc structure; (d) bcc structure; (e) rhomb structure.











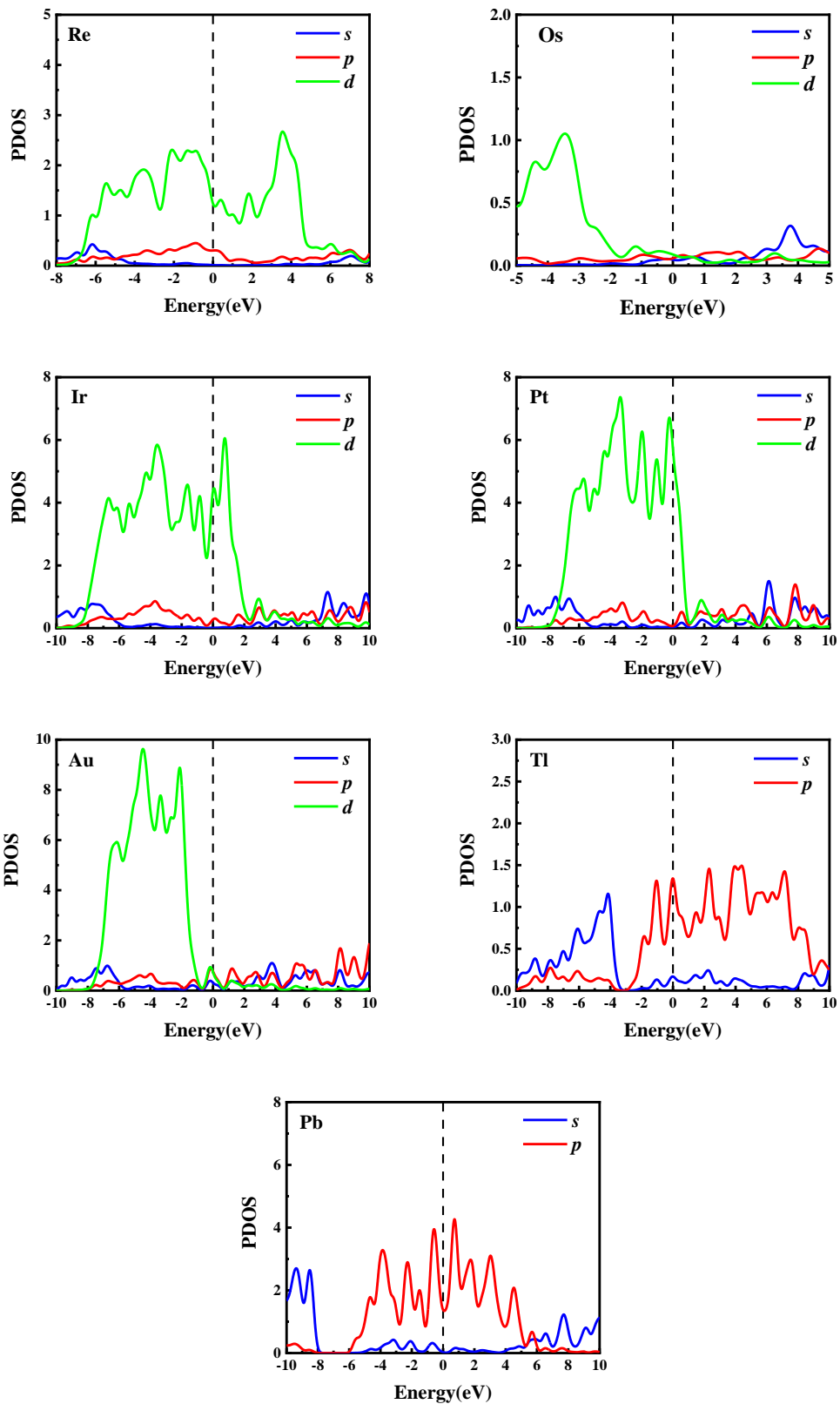


Fig. 2 Partial density of states (PDOS) of the s -, p - and d - orbitals of metallic and semi-metallic elements.

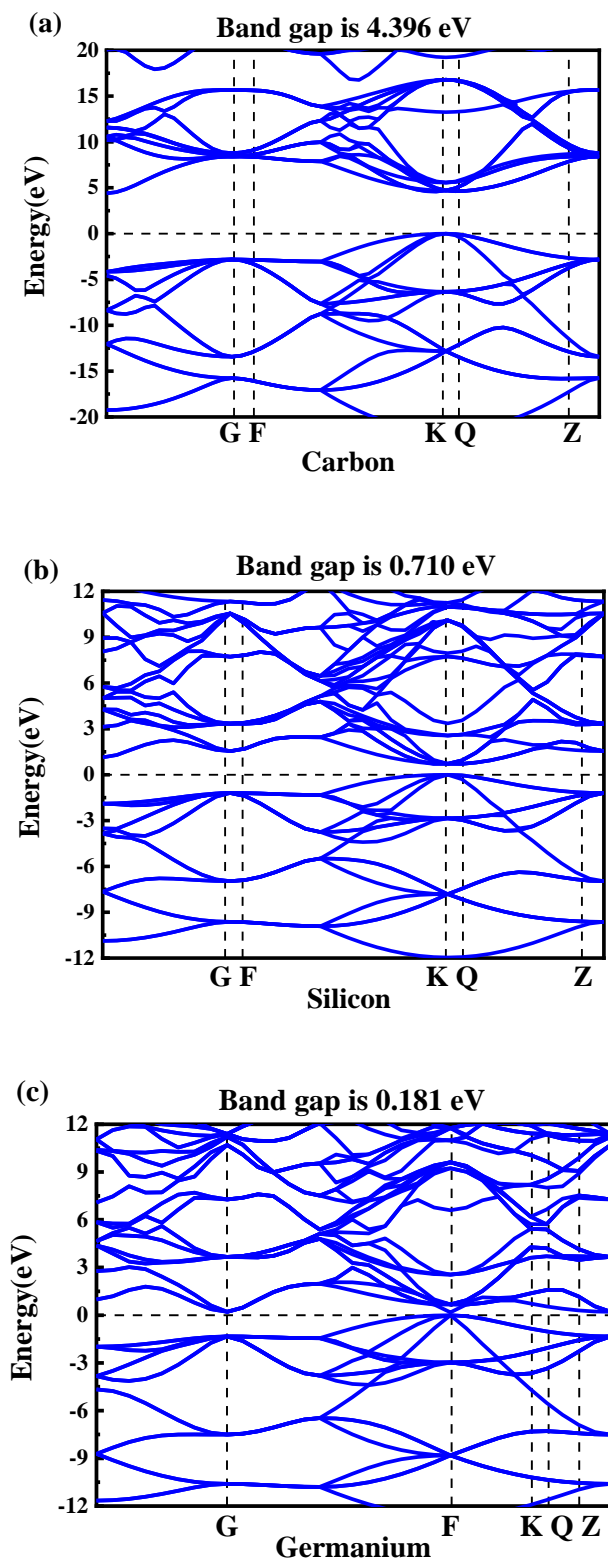
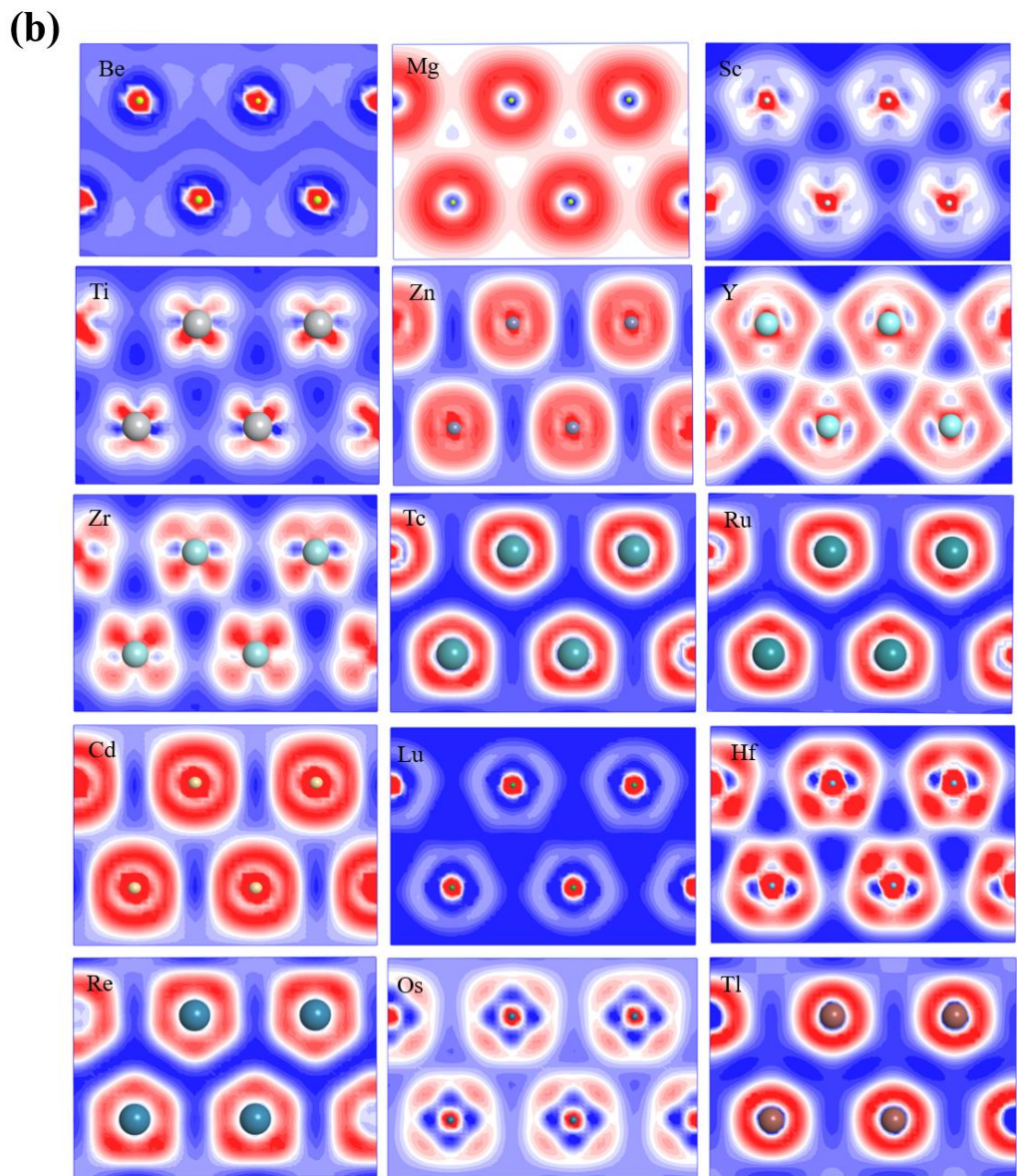
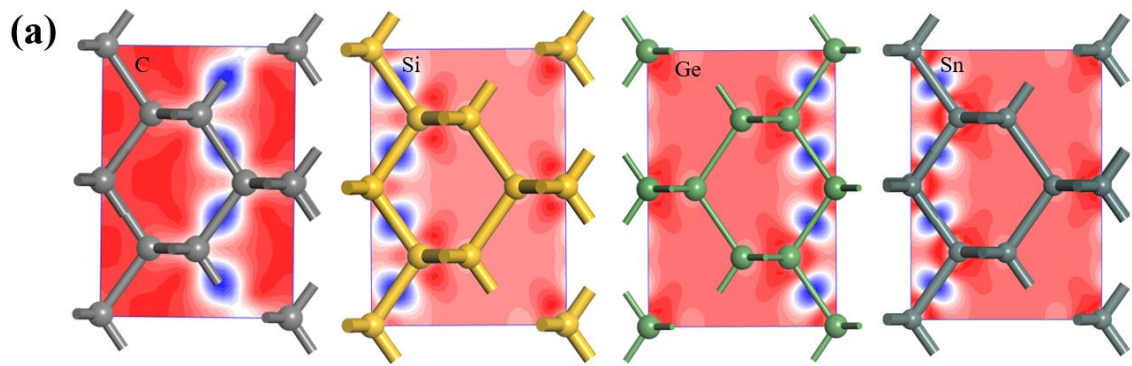
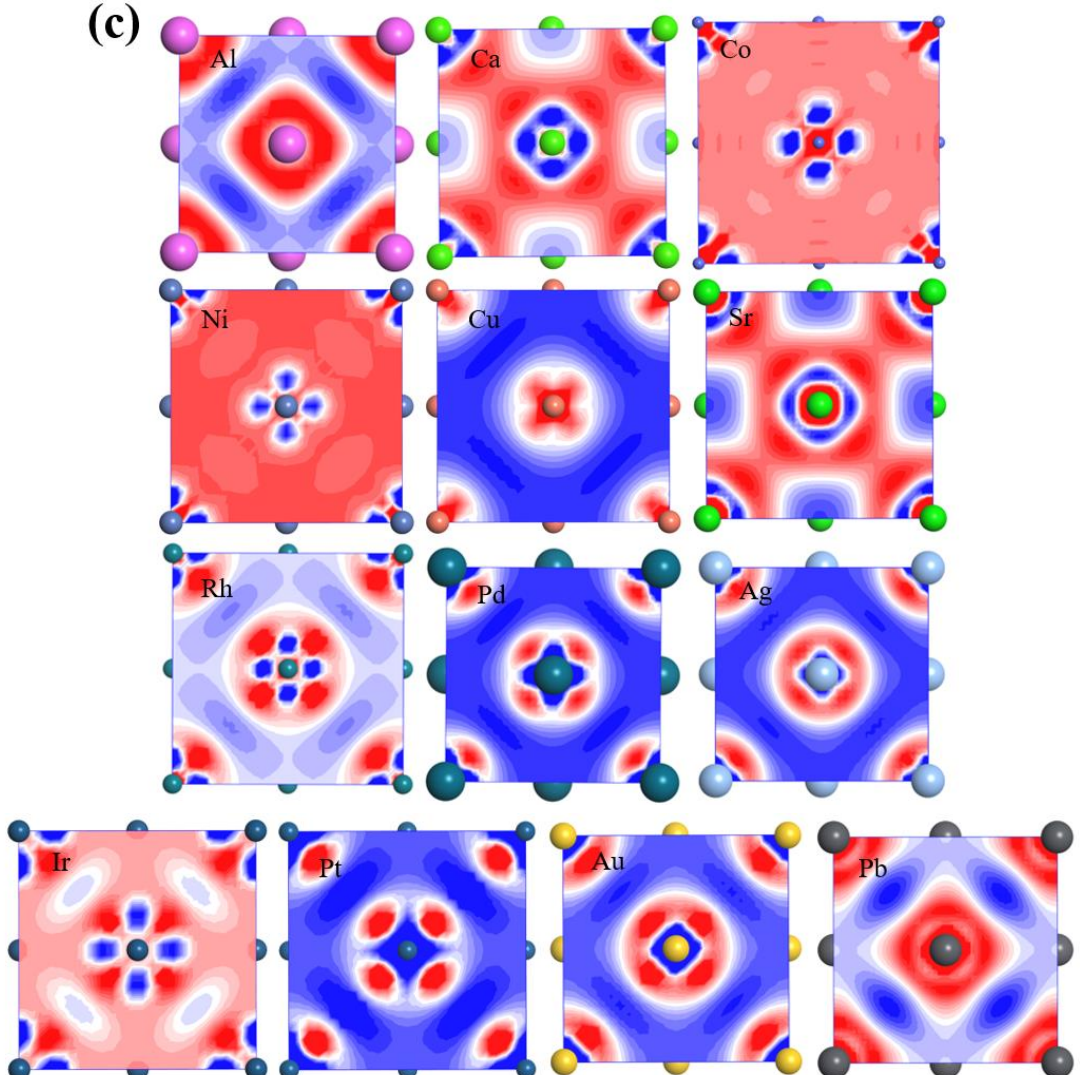
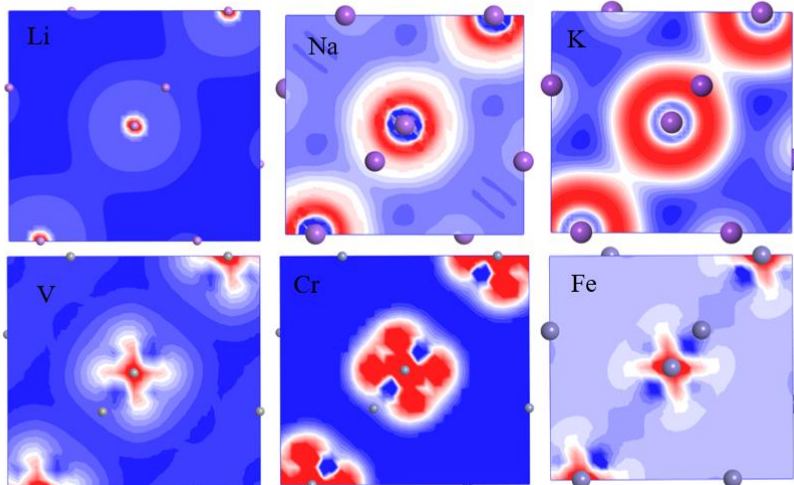


Fig. 3 Band structure of C, Si, and Ge (semi-metals).



(c)**(d)**

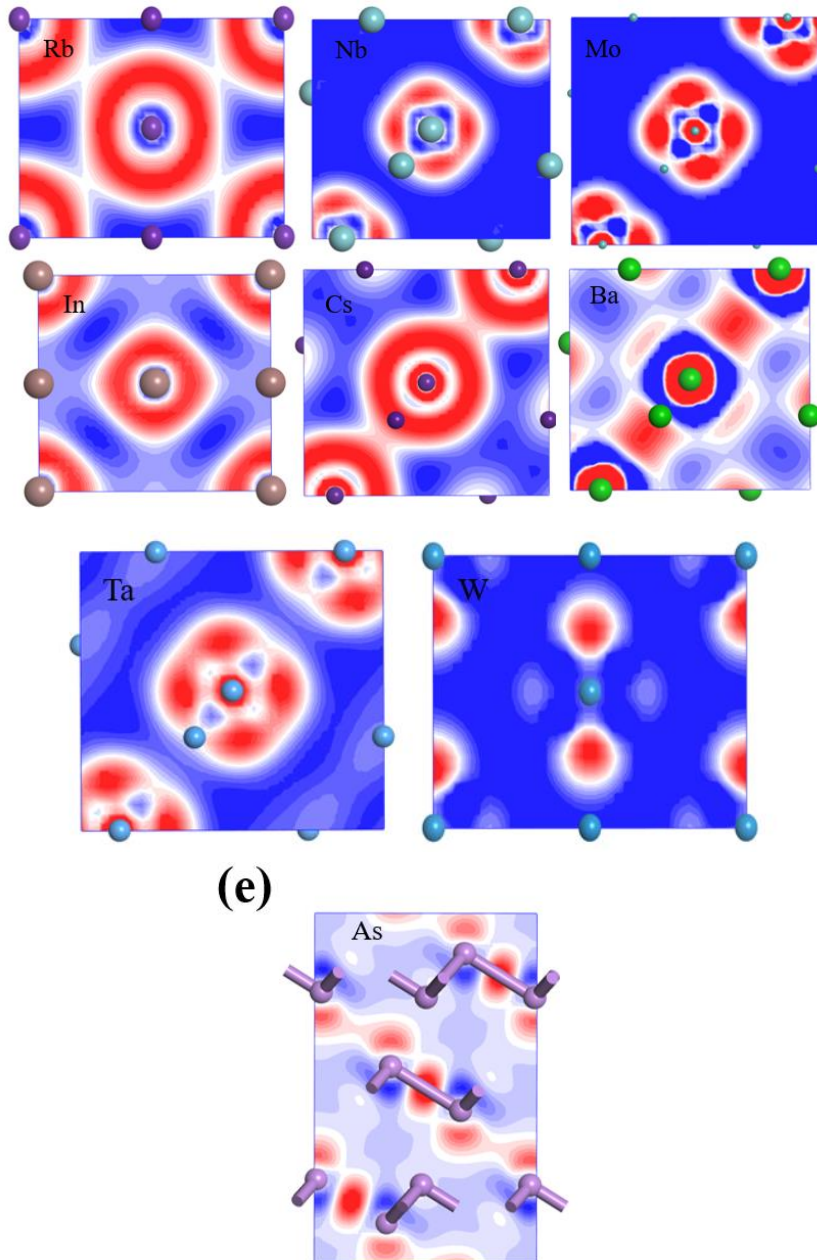


Fig. 4 Deformation charge-density diagrams of (a) diamond-structure elements, (b) hcp structure elements, (c) fcc structure elements, (d) bcc structure elements, and (e) rhomb-structure elements. The blue and red areas represent the concentration and decrease of electrons, respectively.

1	2													18				
1 H 31	2													2 He 28				
3 Li 128 -0.728	4 Be 96 -8.892																	
11 Na 166 -0.539	12 Mg 128 -6.480																	
19 K 203 -0.233	20 Ca 128 -3.547																	
37 Rb 220 -0.224	38 Sr 195 -2.227																	
55 Cs 244 -0.210	56 Ba 215 -1.480	57-70 *	71 Lu 187 -4.665	72 Hf 175 -15.459	73 Ta 170 -29.192	74 W 162 -31.164	75 Re 151 -27.879	76 Os 144 -21.370	77 Ir 141 -22.043	78 Pt 136 -13.672	79 Au 136 -10.771	80 Hg 132 -11.771	81 Tl 145 -1.023	82 Pb 146 -0.493	83 Bi 148 ---	84 Po 140 ---	85 At 150 ---	86 Rn 150 ---
87 Er 260	88 Ra 221	89-102 **	103 Lr --	104 Rf --	105 Db --	106 Sg --	107 Bh --	108 Hs --	109 Mt --	110 Ds --	111 Rg --	112 Cn --	113 Uut --	114 Uuq --	115 Uup --	116 Uuh --	117 Uus --	118 Uuo --

Atomic # → 47
 Symbol → Ag
 Atomic radius (picometers) → 145
 Deformation charge-bond energy (%) → -12.324
Ag ←

Fig. 5 The deformation charge-bond energy $\Delta V_{bc} \left(\vec{r} - \vec{r}' \right)$ values of 47 metals and semi-metals, with their positions in the periodic table.

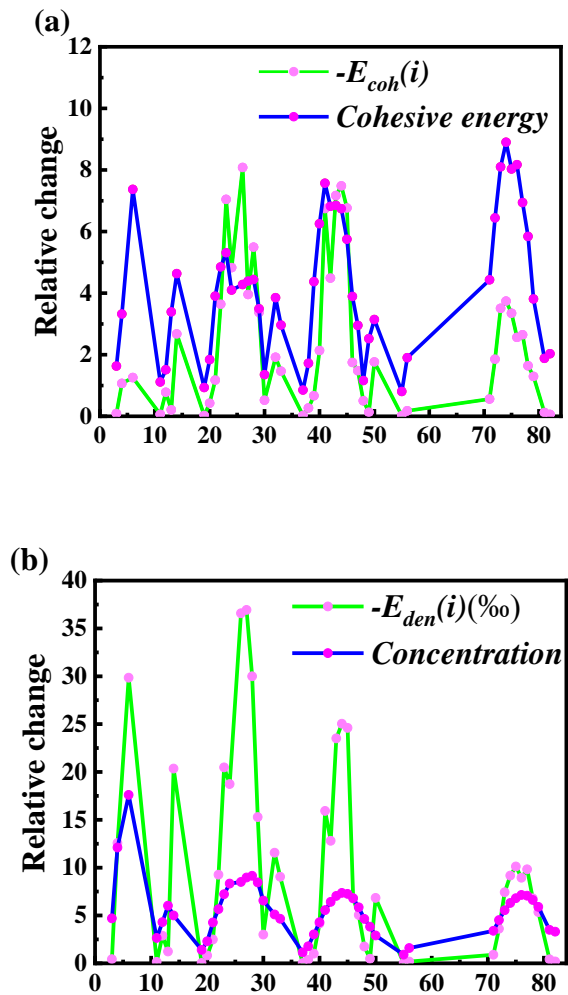


Fig. 6 (a) deformation atomic cohesive energy - $\Delta E_{coh}(i)$ (eV) and atomic cohesive energy(eV/atom), (b) deformation bond energy density - $\Delta E_{den}(i)$ ($eV \cdot \text{\AA}^{-3}$) and atomic concentration(10^{28}m^{-3}). Atomic concentration and cohesive energies value are from the ref[28].

Table 1 Lattice parameters of metallic and semi-metallic elements.

Element	Angle			Lattice parameters		
	α	β	γ	$a (\text{\AA})$	$b (\text{\AA})$	$c (\text{\AA})$
Li	90°	90°	90°	3.509	3.509	3.509
Na	90°	90°	90°	4.291	4.291	4.291
K	90°	90°	90°	5.320	5.320	5.320
Rb	90°	90°	90°	5.700	5.700	5.700
Cs	90°	90°	90°	6.140	6.140	6.140
Be	90°	90°	120°	2.286	2.286	3.583
Mg	90°	90°	120°	3.209	3.209	5.211
Ca	90°	90°	90°	5.582	5.582	5.582
Sr	90°	90°	90°	6.085	6.085	6.085
Ba	90°	90°	90°	5.019	5.019	5.019
Sc	90°	90°	120°	3.308	3.308	5.265
Y	90°	90°	120°	3.645	3.645	5.731
Lu	90°	90°	120°	3.505	3.505	5.549
Ti	90°	90°	120°	2.951	2.951	4.679
Zr	90°	90°	120°	3.231	3.231	3.231
Hf	90°	90°	120°	3.195	3.195	5.051
V	90°	90°	90°	3.028	3.028	3.028
Nb	90°	90°	90°	3.301	3.301	3.301
Ta	90°	90°	90°	3.303	3.303	3.303
Cr	90°	90°	90°	2.885	2.885	2.885
Mo	90°	90°	90°	3.147	3.147	3.147
W	90°	90°	90°	3.165	3.165	3.165
Tc	90°	90°	120°	2.735	2.735	4.388
Re	90°	90°	120°	2.760	2.760	4.458
Fe	90°	90°	90°	2.866	2.866	2.866

Ru	90°	90°	120°	2.706	2.706	4.282
Os	90°	90°	120°	2.735	2.735	2.735
Co	90°	90°	90°	3.544	3.544	3.544
Rh	90°	90°	90°	3.804	3.804	3.804
Ir	90°	90°	90°	3.839	3.839	3.839
Ni	90°	90°	90°	3.524	3.524	3.524
Pd	90°	90°	90°	3.891	3.891	3.891
Pt	90°	90°	90°	3.924	3.924	3.924
Cu	90°	90°	90°	3.615	3.615	3.615
Ag	90°	90°	90°	4.086	4.086	4.086
Au	90°	90°	90°	4.078	4.078	4.078
Zn	90°	90°	120°	2.665	2.665	4.947
Cd	90°	90°	120°	2.979	2.979	5.617
Al	90°	90°	90°	4.050	4.050	4.050
In	90°	90°	90°	3.252	3.252	4.951
Tl	90°	90°	120°	4.457	4.457	5.525
C	90°	90°	90°	3.567	3.567	3.567
Si	90°	90°	90°	5.431	5.431	5.431
Ge	90°	90°	90°	5.658	5.658	5.658
Sn	90°	90°	90°	6.491	6.491	6.491
Pb	90°	90°	90°	4.950	4.950	4.950
As	90°	90°	120°	3.760	3.760	3.760

Table 2 Cut-off energies and k -points of metallic and semi-metallic elements.

Element	Cut-off energy	k -point
Li	544.2 eV	$8 \times 8 \times 8$
Na	598.7 eV	$6 \times 6 \times 6$
K	435.4 eV	$6 \times 6 \times 6$
Rb	250.3 eV	$4 \times 4 \times 4$
Cs	136.1 eV	$4 \times 4 \times 4$
Be	571.4 eV	$13 \times 13 \times 8$
Mg	479.8 eV	$9 \times 9 \times 6$
Ca	326.5 eV	$4 \times 4 \times 4$
Sr	272.1 eV	$4 \times 4 \times 4$
Ba	190.5 eV	$6 \times 6 \times 6$
Sc	410.9 eV	$9 \times 9 \times 6$
Y	272.1 eV	$8 \times 8 \times 4$
Lu	408.2 eV	$8 \times 8 \times 6$
Ti	381.0 eV	$10 \times 10 \times 6$
Zr	272.1 eV	$9 \times 9 \times 6$
Hf	435.4 eV	$9 \times 9 \times 6$
V	381.0 eV	$8 \times 8 \times 8$
Nb	400.0 eV	$8 \times 8 \times 8$
Ta	359.2 eV	$8 \times 8 \times 8$
Cr	381.0 eV	$10 \times 10 \times 10$
Mo	421.8 eV	$8 \times 8 \times 8$
W	353.7 eV	$8 \times 8 \times 8$
Tc	419.1 eV	$11 \times 11 \times 6$
Re	347.3 eV	$10 \times 10 \times 6$
Fe	353.7 eV	$10 \times 10 \times 10$
Ru	449.0 eV	$11 \times 11 \times 6$
Os	370.1 eV	$11 \times 11 \times 6$
Co	381.0 eV	$8 \times 8 \times 8$
Rh	549.7 eV	$8 \times 8 \times 8$
Ir	326.5 eV	$8 \times 8 \times 8$
Ni	400.0 eV	$8 \times 8 \times 8$
Pd	560.6 eV	$6 \times 6 \times 6$
Pt	321.1 eV	$6 \times 6 \times 6$
Cu	408.2 eV	$8 \times 8 \times 8$
Ag	517.0 eV	$6 \times 6 \times 6$
Au	321.1 eV	$6 \times 6 \times 6$
Zn	394.6 eV	$11 \times 11 \times 6$
Cd	299.3 eV	$10 \times 10 \times 4$
Al	190.5 eV	$6 \times 6 \times 6$
In	326.5 eV	$8 \times 8 \times 5$

Tl	340.1 eV	$8 \times 8 \times 6$
C	400.0 eV	$8 \times 8 \times 8$
Si	190.5 eV	$6 \times 6 \times 6$
Ge	394.6 eV	$4 \times 4 \times 4$
Sn	312.9 eV	$4 \times 4 \times 4$
Pb	285.7 eV	$6 \times 6 \times 6$
As	408.2 eV	$8 \times 8 \times 2$

Table 3 BBC model values of deformation charge density $\delta\rho(\vec{r})$ and deformation charge-bond energy $\Delta V_{bc}(\vec{r} - \vec{r}')$

$$(\varepsilon_0 = 8.85 \times 10^{-12} C^2 N^{-1} m^{-2}, e = 1.60 \times 10^{-19} C, |\vec{r} - \vec{r}'| = r_s)$$

Element	Bonding-electron density $\delta\rho(r) \left(e / \text{\AA}^3 \right)$	Hole-electron density $\delta\rho(r') \left(e / \text{\AA}^3 \right)$	Electronic radius $r_s(\text{\AA})$	Deformation charge-bond energy $\Delta V_{bc}(\vec{r} - \vec{r}')(eV)$
Li	0.0050	-0.0581	1.28	-7.281×10^{-3}
Na	0.0046	-0.0128	1.66	-5.393×10^{-3}
K	0.0028	-0.0032	2.03	-2.328×10^{-3}
Rb	0.0021	-0.0029	2.20	-2.242×10^{-3}
Cs	0.0019	-0.0018	2.44	-2.098×10^{-3}
Be	0.0624	-0.2431	0.96	-8.892×10^{-2}
Mg	0.0318	-0.0508	1.41	-6.479×10^{-2}
Ca	0.0259	-0.0113	1.76	-3.547×10^{-2}
Sr	0.0144	-0.0075	1.95	-2.227×10^{-2}
Ba	0.0060	-0.0073	2.15	-1.480×10^{-2}
Sc	0.0153	-0.0626	1.70	-9.779×10^{-2}
Y	0.0129	-0.0241	1.90	-5.555×10^{-2}
Lu	0.0032	-0.0887	1.87	-4.665×10^{-2}
Ti	0.0338	-0.1188	1.60	-3.034×10^{-1}
Zr	0.0258	-0.0582	1.75	-1.779×10^{-1}

Hf	0.0256	-0.0512	1.75	-1.546×10^{-1}
V	0.0441	-0.2206	1.53	-5.868×10^{-1}
Nb	0.0454	-0.1447	1.64	-5.619×10^{-1}
Ta	0.0394	-0.0724	1.70	-2.919×10^{-1}
Cr	0.0527	-0.2047	1.39	-4.023×10^{-1}
Mo	0.0423	-0.1421	1.54	-3.740×10^{-1}
W	0.0183	-0.2120	1.62	-3.116×10^{-1}
Tc	0.0726	-0.1667	1.47	-5.975×10^{-1}
Re	0.0528	-0.0935	1.51	-2.788×10^{-1}
Fe	0.1160	-0.2014	1.32	-6.731×10^{-1}
Ru	0.0769	-0.1699	1.46	-6.234×10^{-1}
Os	0.0528	-0.0908	1.44	-2.137×10^{-1}
Co	0.2568	-0.1008	1.26	-5.911×10^{-1}
Rh	0.1079	-0.1259	1.42	-5.637×10^{-1}
Ir	0.0995	-0.0552	1.41	-2.204×10^{-1}
Ni	0.2927	-0.0741	1.24	-4.575×10^{-1}
Pd	0.0189	-0.2056	1.39	-1.457×10^{-1}
Pt	0.0383	-0.1067	1.36	-1.367×10^{-1}
Cu	0.0458	-0.2130	1.32	-2.812×10^{-1}
Ag	0.0301	-0.0888	1.45	-1.232×10^{-1}
Au	0.0377	-0.0854	1.36	-1.077×10^{-1}
Zn	0.0354	-0.0632	1.22	-4.353×10^{-2}
Cd	0.0274	-0.0343	1.44	-4.189×10^{-2}
Al	0.0219	-0.0428	1.21	-1.754×10^{-2}
In	0.0102	-0.0258	1.42	-1.101×10^{-2}
Tl	0.0099	-0.0223	1.45	-1.023×10^{-2}
C	0.4272	-0.1346	0.76	-1.048×10^{-1}
Si	0.1857	-0.0989	1.11	-2.227×10^{-1}
Ge	0.1477	-0.0600	1.20	-1.597×10^{-1}

Sn	0.1003	-0.0392	1.39	-1.468×10^{-1}
Pb	0.0077	-0.0133	1.46	-4.926×10^{-3}
As	0.0843	-0.0843	1.19	-1.219×10^{-1}

Table 4 Deformation atomic cohesive energies $\Delta E_{\text{coh}}(i)$ and deformation bonding energy densities $\Delta E_{\text{den}}(i)$ from Eq. 30.

Element	$\Delta V_{bc}(\vec{r} - \vec{r}')(eV)$	$\Delta E_{\text{coh}}(i)(eV)$	$\Delta E_{\text{den}}(i) \left(eV \cdot \dot{\text{A}}^{-3} \right)$
Li	-7.281×10^{-3}	-0.08737	-4.340×10^{-4}
Na	-5.393×10^{-3}	-0.06472	-1.474×10^{-4}
K	-2.328×10^{-3}	-0.02794	-3.479×10^{-5}
Rb	-2.242×10^{-3}	-0.02691	-2.632×10^{-5}
Cs	-2.098×10^{-3}	-0.02517	-1.805×10^{-5}
Be	-8.892×10^{-2}	-1.06707	-1.256×10^{-2}
Mg	-6.479×10^{-2}	-0.77754	-2.889×10^{-3}
Ca	-3.547×10^{-2}	-0.42560	-8.132×10^{-4}
Sr	-2.227×10^{-2}	-0.26718	-3.753×10^{-4}
Ba	-1.480×10^{-2}	-0.17762	-1.862×10^{-4}
Sc	-9.779×10^{-2}	-1.17334	-2.478×10^{-3}
Y	-5.555×10^{-2}	-0.66659	-1.012×10^{-3}
Lu	-4.665×10^{-2}	-0.55980	-8.917×10^{-4}
Ti	-3.034×10^{-1}	-3.64035	-9.258×10^{-3}
Zr	-1.779×10^{-1}	-2.13446	-4.149×10^{-3}
Hf	-1.546×10^{-1}	-1.85502	-3.605×10^{-3}
V	-5.868×10^{-1}	-7.04108	-2.047×10^{-2}
Nb	-5.619×10^{-1}	-6.74242	-1.592×10^{-2}
Ta	-2.919×10^{-1}	-3.50301	-7.427×10^{-3}
Cr	-4.023×10^{-1}	-4.82818	-1.873×10^{-2}

Mo	-3.740×10^{-1}	-4.48753	-1.280×10^{-2}
W	-3.116×10^{-1}	-3.73970	-9.163×10^{-3}
Tc	-5.975×10^{-1}	-7.16953	-2.351×10^{-2}
Re	-2.788×10^{-1}	-3.34544	-1.012×10^{-2}
Fe	-6.731×10^{-1}	-8.07740	-3.658×10^{-2}
Ru	-6.234×10^{-1}	-7.48110	-2.504×10^{-2}
Os	-2.137×10^{-1}	-2.5644	-8.946×10^{-3}
Co	-5.911×10^{-1}	-7.09284	-3.693×10^{-2}
Rh	-5.637×10^{-1}	-6.76473	-2.461×10^{-2}
Ir	-2.204×10^{-1}	-2.64510	-9.829×10^{-3}
Ni	-4.575×10^{-1}	-5.48977	-2.999×10^{-2}
Pd	-1.457×10^{-1}	-1.74797	-6.778×10^{-3}
Pt	-1.367×10^{-1}	-1.64065	-6.794×10^{-3}
Cu	-2.812×10^{-1}	-3.37455	-1.528×10^{-2}
Ag	-1.232×10^{-1}	-1.47884	-5.053×10^{-3}
Au	-1.077×10^{-1}	-1.29253	-5.352×10^{-3}
Zn	-4.353×10^{-2}	-0.52233	-2.996×10^{-3}
Cd	-4.189×10^{-2}	-0.50271	-1.754×10^{-3}
Al	-1.754×10^{-2}	-0.21049	-1.238×10^{-3}
In	-1.101×10^{-2}	-0.13209	-4.805×10^{-4}
Tl	-1.023×10^{-2}	-0.12279	-4.195×10^{-4}
C	-1.048×10^{-1}	-1.25781	-2.985×10^{-2}
Si	-2.227×10^{-1}	-2.67258	-2.036×10^{-2}
Ge	-1.597×10^{-1}	-1.91645	-1.155×10^{-2}
Sn	-1.468×10^{-1}	-1.76159	-6.833×10^{-3}
Pb	-4.926×10^{-3}	-0.05911	-1.978×10^{-4}
As	-1.219×10^{-1}	-1.46319	-9.045×10^{-3}